Observation of Transport to Thermal Equilibrium in Pure Electron Plasmas

C. F. Driscoll, J. H. Malmberg, and K. S. Fine
Department of Physics, University of California, San Diego, La Jolla, California 92093
(Received 16 November 1987)

Transport of magnetically confined pure electron plasmas to global thermal equilibrium has recently been observed. In equilibrium, the $\mathbf{E}\times\mathbf{B}$ and diamagnetic drifts calculated from the measured temperature and density profiles combine to give rigid rotation (i.e., $\langle v_\theta \rangle = \omega r$), as expected. However, the density profile relaxes towards equilibrium up to 5000 times faster than predicted by Boltzmann transport theory: Over a decade range of magnetic field, the density equilibration time is always less than predicted, and scales as B^1 rather than as B^4.

PACS numbers: 52.25.Fi, 52.25.Wz

Charged-particle traps are widely used to study plasma wave, transport, and equilibrium properties,[1-7] to measure the fundamental[8-10] or chemical[11] properties of particles, and to store or manipulate particles for various technologies.[12,13] These devices have been used to contain electrons,[1-4,6,8] ions of one or more species,[5,7,10,11] positrons,[13] and antiprotons,[9,10] with the number of trapped particles varying from 1 to 10^{10} or more. In these traps, a uniform axial magnetic field $B\hat{\mathbf{z}}$ provides radial confinement, and voltages applied to the end electrodes provide axial confinement. In the present experiment, the contained plasma is an elongated spheroid, rotating about the axis of symmetry because of the radial electric field arising from the totally unneutralized charges.

Many applications rely on an exceptional property of unneutralized plasmas, namely, that the plasma can relax to global thermal equilibrium and still remain confined. The plasma may be thought of as an isolated system of N classical particles interacting with the apparatus only through stationary, azimuthally symmetric fields. In this idealization, the total energy H and the total angular momentum P_θ of the plasma are conserved quantities. Interparticle interactions will, in general, cause internal transport of particles and energy until the plasma reaches the maximal entropy state consistent with the given (N,H,P_θ), i.e., global thermal equilibrium. The equilibrium may be a plasma, liquid, or crystal state, depending on the temperature.[3,7]

Since both H and P_θ are conserved, they enter the thermal equilibrium partition function on an equal footing,[2,3,14,15] as $\exp[-(H-\omega_{\rm eq}P_\theta)/kT_{\rm eq}]$. In the plasma regime of interest here, the particles are uncorrelated, and the equilibrium velocity distribution is a Maxwellian at temperature $T_{\rm eq}$, superimposed on a "rigid" average rotation given by $\langle v_\theta \rangle = \omega_{\rm eq} r$.[15] The equilibrium density is given by

$$n(\mathbf{r}) = n_{\rm eq}\exp\{-[q\phi(\mathbf{r}) + \alpha r^2]/kT_{\rm eq}\}, \qquad (1)$$

where $\alpha \equiv \frac{1}{2}m(\Omega\,|\,\omega_{\rm eq}\,| - \omega_{\rm eq}^2)$. The equilibria are parametrized by the three constants ($n_{\rm eq}$, $\omega_{\rm eq}$, and $T_{\rm eq}$) which are determined by N, H, and P_θ. Here, $\Omega \equiv |\,q\,|B/mc$ is the cyclotron frequency, $\mathbf{r} \equiv (r,\theta,z)$, and the potential $\phi(\mathbf{r})$ is determined by Poisson's equation. The density of Eq. (1) is uniform to within a few Debye lengths of the plasma edges, after which the density falls exponentially.[16]

In this paper, we report observations of pure-electron-plasma equilibria, and quantify the rate at which electron-electron interactions cause particle transport across the magnetic field, towards the confined equilibrium state. When first captured, the plasma is generally not near thermal equilibrium, although it would be a stable dynamical equilibrium in the absence of collisions. Electron-electron collisions first cause the thermal-velocity distribution to become Maxwellian along each field line separately; this has been measured previously, and is found to occur on the time scale of $\nu_{\rm th}^{-1} \simeq 4$ msec.[17] On a longer time scale of interest here, electron-electron interactions cause transport of heat and particles across the magnetic field: The temperature becomes uniform, and the density profile becomes such as to produce rigid drift rotation of the plasma. This equilibration time $\tau_{\rm eq}$ will be seen to be seconds in our apparatus. On a yet longer time scale, weak external couplings which break azimuthal symmetry cause P_θ to change, causing radial expansion and loss of plasma to the walls. At base pressures of 5×10^{-11} Torr, we obtain empirical plasma expansion (or "mobility") times τ_m scaling as[6]

$$\tau_m = (130\ {\rm sec})[B/(100\ {\rm G})]^2[L_p/(5\ {\rm cm})]^{-2}.$$

For the present experiment, we utilize axially short plasmas so that $\tau_m \gg \tau_{\rm eq}$, in which case most effects from the weak asymmetries can be ignored.

The plasmas are contained in a cylindrical apparatus, as shown schematically in Fig. 1. The apparatus is operated in an inject, hold, and dump-and-measure cycle. For injection, cylinder A is briefly grounded, resulting in a column of electrons from the negatively biased filament to cylinder C. When a negative voltage is applied to cylinder A, the plasma is trapped within cylinder

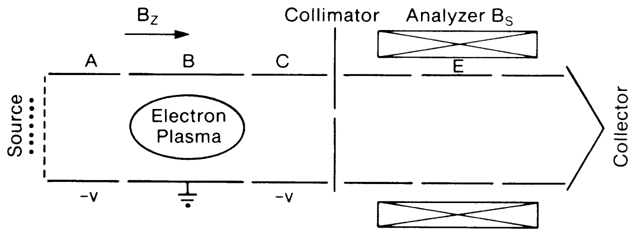

FIG. 1. The cylindrical containment apparatus.

B. For all data presented here, cylinder B had equal length and diameter of 7.6 cm, and the containment voltages were -80 V. The plasmas typically have densities $n \simeq 1\times 10^7$ cm^{-3} and temperatures $kT \simeq 0.8$ eV, with diameters $\simeq 4$ cm and lengths $L_p \simeq 5$ cm. After a containment time t, cylinder C is pulsed to ground potential, and the electrons stream along the magnetic field to the collimator, velocity analyzer, and collector. Repetition of the cycle with varying containment times t and with the collimator hole at varying radii r allows us to construct the time evolution of the plasma. Typically, shot-to-shot variations in the charge collected at any radius are less than 1%. This lack of variation indicates that the plasma is rotationally quite symmetric, and we assume $\partial/\partial\theta = 0$ throughout this paper.

Our basic density measurement is the total charge $Q(r,t)$ which exits along a field line at radius r and passes through the collimator hole of area $A_h = 7.9$ mm^2. This is the z integral of the plasma density, i.e., $Q(r) = qA_h \int dz\, n(r,z)$. To obtain $n(r,z)$, we assume

$$n(r,z) = n(r,0)\exp\{-q[\phi(r,z)-\phi(r,0)]/kT(r)\},$$

since for $t \gg v_{\text{th}}^{-1}$ the plasma is in local thermal equilibrium along each line separately. The measured $Q(r)$ essentially determines the unknown $n(r,0)$. More specifically, we solve Poisson's equation in (r,z) to obtain the self-consistent $n(r,z)$ and $\phi(r,z)$, given the measured $Q(r)$, $T(r)$, and wall potentials $\phi(R_w,z)$. Typically, $Q(r)$ is measured at fifty different radii, $T(r)$ is measured at twelve radii, and Poisson's equation is solved on a 128×128 grid.

We measure the temperature $T(r,t)$ of the plasma by performing parallel-energy discrimination on the dumped electrons as they pass through a secondary axial magnetic field B_s.[17] The additional field B_s changes the parallel energy of each exiting electron by an amount $\Delta E_\parallel = (1-\gamma)E_\perp$, where $\gamma \equiv (B_s+B)/B$ and $E_\perp$ is the perpendicular energy of the electron in the plasma. We obtain the temperature $T \equiv \langle E_\perp \rangle /k$ by measuring the variation in the collected charge $Q(V_E,\gamma)$ as γ and the analyzer voltage V_E are varied. We typically take sufficient data at each radius so that a statistical evaluation of the variations gives T to an accuracy of $\pm 10\%$

The plasma rotation rate $\omega_R(r,z,t)$ can be computed from the experimental data, as the sum of $\mathbf{E}\times\mathbf{B}$ and diamagnetic (or pressure) drifts:

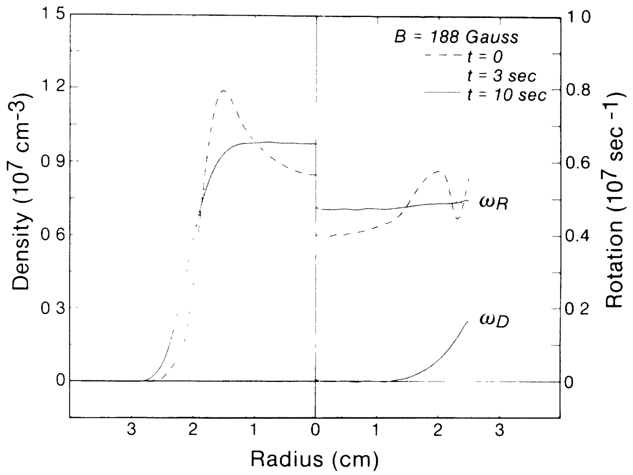

FIG. 2. Experimental plasma density profiles $n(r,t)$ and rotation profiles $\omega_R(r,t)$ at three different times t, showing the evolution to equilibrium. Also shown is the diamagnetic drift $\omega_D(r)$ at $t=10$ sec.

$$\omega_R(r,z,t) \equiv \omega_E(r,z,t) + \omega_D(r,z,t) = \frac{c}{rB}\frac{\partial\phi}{\partial r} + \frac{c}{rBqn}\frac{\partial}{\partial r}(nkT). \tag{2}$$

One can deduce from Eq. (1) that $\omega_R(r,z) = \omega_{\text{eq}}$ in thermal equilibrium. In general, there will be radial shears; but the rotation is quite uniform in z, since $\partial\phi/\partial z \approx 0$ in the body of the plasma, and the assumption of local equilibrium and Eq. (1) imply

$$\frac{\partial\omega_R}{\partial z} = \frac{1}{rT}\frac{\partial T}{\partial r}\frac{\partial\phi}{\partial z}.$$

For simplicity, we consider here only the central radial profiles, i.e., $n(r,0,t)$ and $\omega_R(r,0,t)$.

We are able to identify unambiguously the approach to global thermal equilibrium, as characterized by the density profile becoming such as to give radially uniform rotation and by the temperature becoming radially uniform. In Fig. 2, we show the experimental density and rotation profiles during a typical evolution. At $t=0$, $n(r)$ is peaked near the edge, and the corresponding $\omega_R(r)$ is also peaked. By $t=3$ sec, one can see that some particles have been transported inward to fill in the center, while others have moved outward; and the rotation profile has smoothed correspondingly. At $t=10$ sec, the plasma is essentially in equilibrium, with $\omega_R(r)$ constant to the accuracy of our measurements. We note that in equilibrium, the diamagnetic drift is about 30% of the total drift at the edge of the plasma.

During this particular evolution, the temperature was initially radially uniform at 0.8 eV, and it remained radially uniform throughout the evolution, but it had risen to 1.1 eV by $t=10$ sec. For a similar evolution at $B=47$ G, the initial temperature varied from 1.3 eV at $r=0$ to

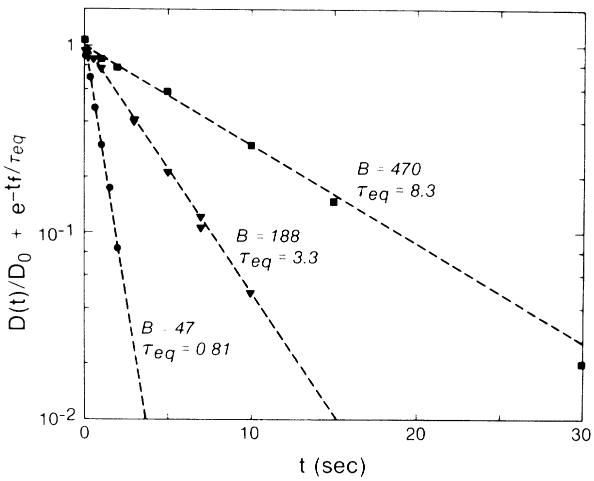

FIG. 3. Measured "distance" from equilibrium $D(t)$ vs time for $B=47$, 188, and 470 G. The dashed lines show exponential fits to obtain τ_{eq}.

2.5 eV at $r=2$ cm; but by $t=1$ sec, the temperature became radially uniform at 2.5 eV to within the 10% accuracy of the diagnostic.

To obtain a characteristic time τ_{eq} for the particle transport towards equilibrium, we focus on the measured $Q(r,t)$ rather than on the derived quantities n and ω_R. We characterize each $Q(r,t)$ by a "distance" from equilibrium $D(t)$, and find that $D(t)$ decreases approximately exponentially with time, giving τ_{eq}. There is no uniquely valid definition of $D(t)$, but we use a linear projection operator which is insensitive to errors in the data. Specifically, from the measured $Q(r,t)$ we calculate $D(t)\equiv\int dr\,\delta Q(r,t)\delta Q(r,0)$, where $\delta Q(r,t)\equiv Q(r,t)-Q(r,t_f)$. Here t_f is a final time large enough so that the profile has essentially reached equilibrium, but small enough that external couplings remain unimportant. Typically, we calculate D for 8–10 experimental profiles taken at different times t. We then obtain τ_{eq} and D_0 as the least-squares fit by

$$D(t)=D_0[\exp(-t/\tau_{eq})-\exp(-t_f/\tau_{eq})].$$

The last term merely corrects for the fact that $D(t)=0$ at $t=t_f$ rather than at $t=\infty$.

Figure 3 shows the experimental $D(t)$ and the exponential fits for three different magnetic fields. The data are well fitted by the exponential curves over the 1- to $1\frac{1}{2}$-decade range of $D(t)$. The three examples shown have $t_f=2$, 10, and 50 sec. In each case, the resulting τ_{eq} is insensitive to the choice for t_f as long as $t_f \gtrsim 2\tau_{eq}$, and we would characterize the accuracy of τ_{eq} as $\pm 25\%$. Other reasonable definitions of D, such as $\tilde{D}(t)\equiv\int dr\,r\delta Q(r,t)\delta Q(r,0)$, give essentially the same results for τ_{eq}. Of course, as is apparent from Fig. 2, the evolution to equilibrium is not just exponential relaxation at all radii; rather, the radial integral in D averages over details of the transport.

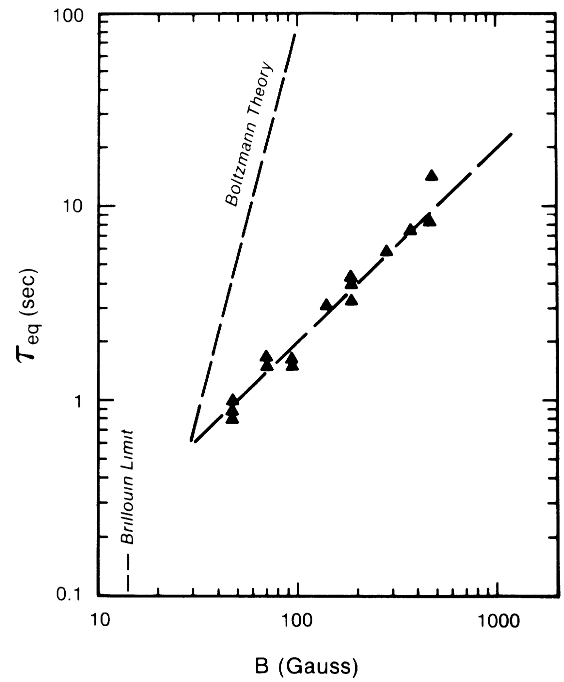

FIG. 4. Experimental density equilibration times τ_{eq} vs magnetic field B. The dashed line through the data represents $\tau_{eq}\propto B^1$; the upper dashed line is the prediction of traditional Boltzmann theory, scaling as B^4.

We have obtained characteristic times τ_{eq} over a range of fields B from 47 to 470 G, as shown in Fig. 4. We find that τ_{eq} scales closely as B^1, implying transport rates scaling as B^{-1}. For this series, we tried to keep the initial plasmas as alike as possible as B was varied. For all but the lowest magnetic fields, the initial $Q(r)$ was uniform out to the plasma edge, after which it dropped sharply; for the lowest fields, $Q(r)$ was more nearly Gaussian. Initial plasma temperatures were typically uniform at about 0.8 eV; however, for the lowest fields, the initial temperature ranged from 1 eV in the center to 2 eV at the edges. For perspective, we note that force-balance considerations give a "Brillouin limit"[2] of $nmc^2 8\pi/B^2 < 1$, or $B > 15$ G at $n=10^7$ cm^{-3}. Our data thus range from 3 to 30 times the minimum field, or from 10^{-1} to 10^{-3} times the maximum density.

These transport results contrast sharply with the predictions of traditional like-particle transport theory.[15,18,19] Local transport theory predicts a particle flux given by

$$\Gamma_r=\frac{-c}{qB}(\nabla\cdot\mathcal{P})_\theta=\frac{c}{qB}\frac{1}{r^2}\frac{\partial}{\partial r}\left[r^2\eta r\frac{\partial}{\partial r}\omega_R(r)\right]. \quad (3)$$

Here, the flux is a radial drift due to θ forces in the stress tensor $\mathcal{P}$; the off-diagonal terms of interest can be expressed as a viscosity coefficient η times the shear in the plasma-rotation velocity. Collisional theory based on the Boltzmann (or Lenard-Balescu) equation gives $\eta = \frac{3}{10} \nu_{th} n m r_L^2$, where

$$\nu_{th} = 4\sqrt{\pi} n q^4 \ln\Lambda / 3\sqrt{m} (kT)^{3/2}$$

is the Spitzer rate of thermal energy equipartition due to collisions,[17,20] and $r_L \equiv (T/m)^{1/2}/\Omega$ is the Larmor radius of electron cyclotron orbits. The effective interaction distance for viscosity is approximately r_L, and the resulting particle fluxes of Eq. (3) scale as B^{-4}, since $\eta \propto B^{-2}$ and $\omega_R \propto B^{-1}$.

The data of Fig. 4 clearly show that Boltzmann theory does not describe the dominant transport occurring in these plasmas. The upper dashed line in Fig. 4 is the exponential relaxation time obtained from Eq. (3), with densities, temperatures, and gradient scales appropriate to this experiment. At high fields, the observed transport to equilibrium occurs 5000 times faster than predicted by this theory. Furthermore, the observed $\tau_{eq} \propto B^1$ scaling strongly disagrees with the B^4 scaling appropriate to this mechanism.

In contrast, recent *nonlocal* transport theories[21-23] consider interactions between electrons separated by distances which are much larger than r_L and which are independent of B. The resulting particle fluxes scale with B as $\nu_{eff} B^{-2}$, where the interaction rate ν_{eff} scales as either B^0, $\ln B$, or B^1, depending on the interaction mechanism considered. The last scaling, which agrees with the present experiments, arises when the bounce-averaged component of the interaction is considered[23] and is closely related to the idealized case of 2D transport of charged rods.[21,22] However, the present data are not sufficiently detailed to verify any one transport mechanism.

In summary, we have observed confined thermal equilibrium plasma states characterized by uniform fluid rotation and uniform temperature. The cross-field particle transport towards equilibrium scales as B^{-1} and is much larger than that predicted by Boltzmann transport theory.

The authors acknowledge useful discussions with Professor Tom O'Neil and Professor Dan Dubin. This work was supported by U.S. Office of Naval Research Contract No. N00014-82K0621.

[1]A. W. Trivelpiece, Comments Plasma Phys. **1**, 57 (1972).

[2]R. C. Davidson, *Theory of Nonneutral Plasmas* (Benjamin, Reading, MA, 1974), Sect. 3.2.

[3]J. H. Malmberg and T. M. O'Neil, Phys. Rev. Lett. **39**, 1333 (1977).

[4]J. S. deGrassie and J. H. Malmberg, Phys. Fluids **23**, 63 (1980).

[5]G. DiMonte, Phys. Rev. Lett. **46**, 26 (1981).

[6]C. F. Driscoll *et al.*, Phys. Fluids **29**, 2015 (1986); C. F. Driscoll and J. H. Malmberg, Phys. Rev. Lett. **50**, 167 (1983).

[7]J. J. Bollinger and D. J. Wineland, Phys. Rev. Lett. **53**, 348 (1984).

[8]R. S. Van Dyck, Jr., *et al.*, in *Atomic Physics, Nine: Proceedings of the Ninth International Conference on Atomic Physics, Seattle, Washington, July 1984*, edited by R. S. Van Dyck, Jr., and E. N. Fortson (World Scientific, Singapore, 1984).

[9]G. Gabrielse *et al.*, Phys. Rev. Lett. **57**, 2504 (1986).

[10]N. Jarmie, Nucl. Instrum. Methods Phys. Res., Sect B **24/25**, 437 (1987).

[11]J. B. Jeffries *et al.*, Int. J. Mass Spectrom. Ion Processes **54**, 169 (1983).

[12]J. J. Bollinger *et al.*, Phys. Rev. Lett. **54**, 1000 (1985); D. J. Larson *et al.*, Phys. Rev. Lett. **57**, 70 (1986).

[13]C. M. Surko *et al.*, Rev. Sci. Instrum. **57**, 1862 (1986).

[14]L. D. Landau and E. M. Lifshitz, *Statistical Mechanics* (Pergamon, London, 1958), Sect. 4.

[15]T. M. O'Neil and C. F. Driscoll, Phys. Fluids **22**, 266 (1979).

[16]S. A. Prasad and T. M. O'Neil, Phys. Fluids **22**, 278 (1979).

[17]A. W. Hyatt, C. F. Driscoll, and J. H. Malmberg, Phys. Rev. Lett. **59**, 2975 (1987).

[18]A. Simon, Phys. Rev. **100**, 1557 (1955).

[19]C. L. Longmire and M. N. Rosenbluth, Phys. Rev. **103**, 507 (1956).

[20]L. Spitzer, Jr., *Physics of Fully Ionized Gasses* (Interscience, New York, 1962), Sect. 5.3.

[21]J. B. Taylor and B. McNamara, Phys. Fluids **14**, 1492 (1971).

[22]H. Okuda and J. M. Dawson, Phys. Fluids **16**, 408 (1973).

[23]T. M. O'Neil, Phys. Rev. Lett. **55**, 943 (1985); D. H. E. Dubin and T. M. O'Neil, preceding Letter [Phys. Rev. Lett. **60**, 1286 (1988)].